TRAJECTORY DESIGN USING A DYNAMICAL SYSTEMS APPROACH WITH APPLICATION TO GENESIS

K. C. Howell*, B. T. Barden†, R. S. Wilson†, and M. W. Lo‡

A number of missions have recently been proposed that aim to take advantage of the growing scientific interest in the region of space near libration points in the Sun-Earth system. In support of missions that include increasingly complex trajectories and incorporate libration point orbits, more efficient techniques and new philosophies for design must be considered. In this work, the proposed GENESIS mission provides an opportunity to demonstrate the usefulness of dynamical systems theory in initiating trajectory design. From there, the methodology used to meet launch and return constraints is presented. Additionally, a method for finding similar solutions with launches in different months is applied to expand the launch opportunities. Finally, the results from a launch period analysis are discussed.

INTRODUCTION

In astrodynamics, the complex missions envisioned for the upcoming decades will demand innovative spacecraft trajectory concepts. It is also increasingly apparent that accomplishment of many short- and long-term science and exploration goals will require a broader view that expands the range of options available. Such is the case with the GENESIS solar wind sample return mission proposed for NASA's Discovery program. The intended science investigations create new demands in mission design. The primary scientific goal is the collection of solar wind particles during an interval of approximately two years. These particles will provide useful information regarding the chemical and isotopic composition of the Sun. This information can then subsequently be used to validate theories concerning the composition of several objects in the solar system, including planetary atmospheres. To successfully collect these particles, the spacecraft must be beyond the magnetosphere of the Earth. On the other hand, to help keep the mission operation costs low, it is desirable that the spacecraft be as close to the Earth as possible. Thus, an L_1 libration point trajectory is the ideal platform for this mission. In addition, the actual scientific analysis of the collected samples is to be performed on Earth. Thus, the trajectory must accommodate the added challenge of returning the spacecraft (with its samples) from the vicinity of L_1 to Earth and then reentering the atmosphere at some set of specified coordinates. To further complicate the trajectory, a day side reentry is required.

While design capabilities for such missions have significantly improved in the last five years, they are still limited. Computational approaches to determine a nominal trajectory are essentially manual numerical searches in a regime where conic approximations are not adequate; standard targeting and optimization strategies based on linear variational methods are sometimes difficult to apply and frequently break down because of the nonlinearities and high sensitivities in the problem. Conventional tools simply do not incorporate any firm theoretical understanding of the multi-body problem and do not offer the flexibility to take further advantage of the dynamical relationships in producing alternative trajectory designs and, thus, new mission options.

Traditionally, trajectory design has been initiated with a baseline mission concept rooted in the two-body problem and conics. Design algorithms built on conics use trajectory arcs from a limited set of possible types, i.e., ellipses, parabolas, and hyperbolas. For missions such as GENESIS, a

* Professor, School of Aeronautics and Astronautics, Purdue University, West Lafayette, IN
† Graduate Student, School of Aeronautics and Astronautics, Purdue University, West Lafayette, IN
‡ Member of Technical Staff, Jet Propulsion Laboratory, California Institute of Technology, Pasadena, CA

baseline concept derived from solutions in the three-body regime is necessary. In this study, dynamical systems theory is utilized to explore solution behavior in phase space, and solution arcs that may be useful for design are isolated. These arcs are then patched together to serve as the initial guess for an algorithm to force a solution that meets specified launch and return constraints. Once a nominal solution is computed, other launch options are investigated.

GENERATING A FIRST GUESS: STABLE/ UNSTABLE MANIFOLDS

There are a number of different ways to compute an acceptable solution that will satisfy the mission constraints. The usefulness and success of each approach will depend, in some fashion, on the initial guess. Traditionally, the initial guess is constructed from known solutions in the two-body problem (in the form of conic sections). Depending on the complexity of the problem and the robustness of the algorithm, a patched conic solution may suffice as a first guess. However, a mission concept that involves the spacecraft spending a significant amount of time in the vicinity of a libration point requires an initial guess based in the three-body problem. Unlike the two-body problem, there are no general analytical solutions in the three-body problem; obtaining a first guess in this region of space is difficult. However, a combination of analytical expressions and numerical techniques from dynamical systems theory (DST) cau be used very effectively to initiate the design process. Of course, without a general solution to this nonlinear problem, extensive numerical analysis is still critically necessary. But clever, less costly solutions are available when knowledge of the solution space is expanded and algorithms that employ DST and the dynamical relationships are developed.

Restricted Problem of Three Bodies

Initially, the Sun and the Earth are assumed to be in circular orbits. While various interesting solutions exist in the circular restricted three-body problem, those of particular interest here are the periodic and quasi-periodic solutions near the collinear libration points. The most general type of motion in this region of space is the set of quasi-periodic Lissajous trajectories. These three-dimensional trajectories densely fill a torus that lies in the center manifold. Under certain conditions, and with proper choice of in-plane and out-of-plane amplitudes, periodic halo orbits emerge. While no complete analytical solution exists, halo orbits can be computed numerically using an analytical approximation[1] as the first guess in a differential corrections procedure. Various examples of such solutions are available in a number of three-body systems[1-7].

Precisely periodic halo orbits do not exist in a more complex model, i.e., one that employs ephemeris data for the positions of the Sun, planets, and moons. Rather, the quasi-periodic Lissajous trajectories can be exploited; these solutions still remain bounded for the time frames of interest. Computation of these trajectories, however, is nontrivial. A trial-and-error type numerical search is possible, but this is highly inefficient and offers little or no control over the characteristics of the final solution. A more efficient method combines analytical approximations with numerical techniques for a fast and flexible algorithm. Using the Richardson and Cary expansion[2] as an initial guess, the algorithm in Howell and Pernicka[7] produces the trajectory that is plotted in Figure 1. Shown here is an example of a Lissajous trajectory near the L_1 (interior) libration point in the Sun-Earth/Moon barycenter three-body system. The dynamic model includes JPL ephemerides (DE202) for the positions of the Sun, Earth, and Moon. Three planar projections appear with the origin in each plot corresponding to the L_1 libration point. The three axes in the figure are defined consistent with the rotating frame typically used in the restricted three-body problem. Thus, the x axis is directed from the larger primary (Sun) to the smaller primary (Earth/Moon barycenter), the y axis is defined in the plane of motion of the primaries and 90° from the x axis, and the z axis completes the right handed frame. The trajectory in the figure is characterized by an A_z = **320,000** km with A_x = 230,000 km and A_y = 745,000 km, where A_i is the amplitude of motion in the i^{th}

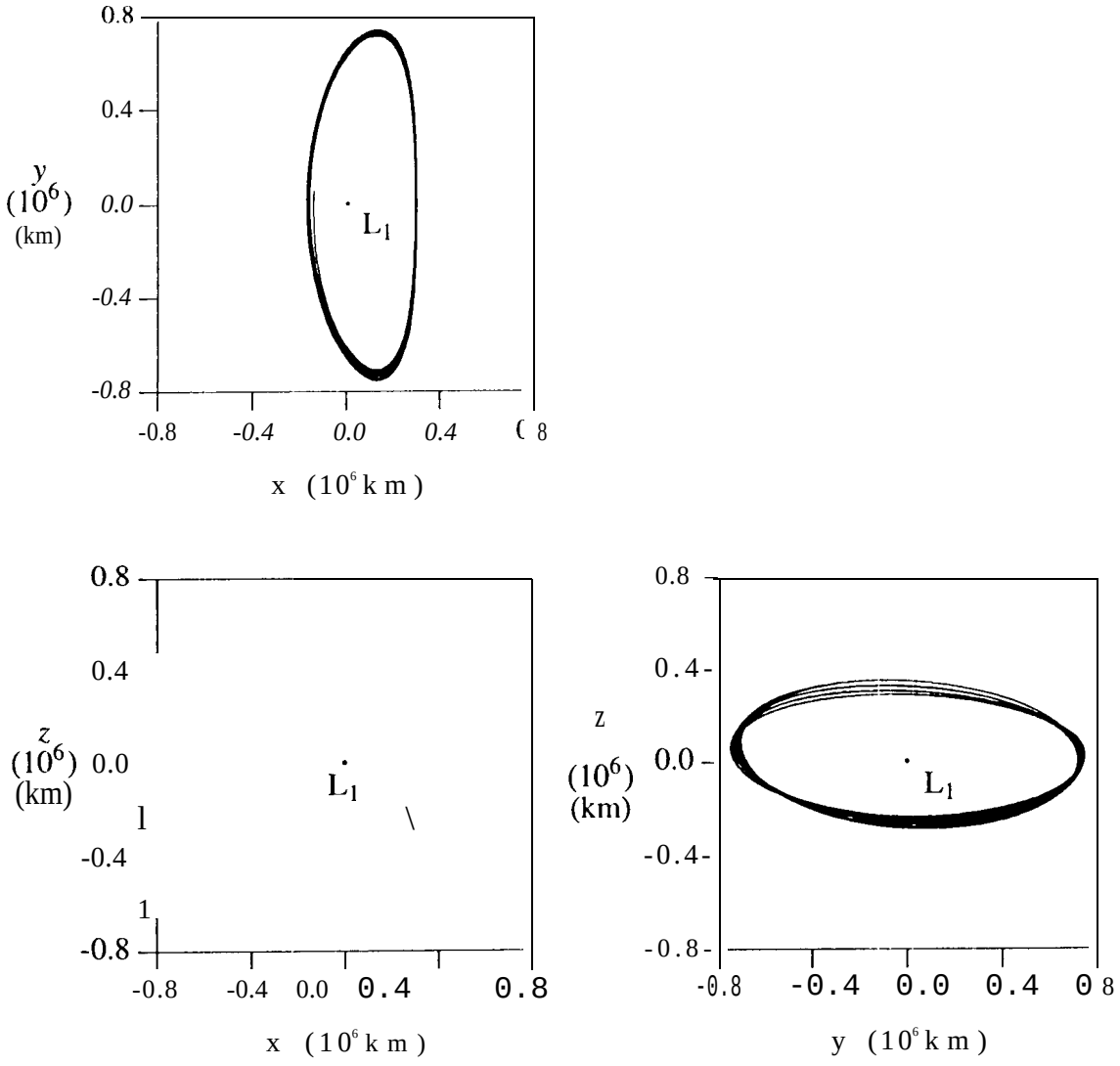

Figure 1 Lissajous Trajectory

direction. The path originates on March 3, 2001 with a total flight time of approximately 1399 days (corresponding to approximately 7.75 revolutions).

Dynamical Systems Theory

Determination of a nominal halo or Lissajous trajectory is only one part of the design process. Transfer trajectories to and from this region of space must also be considered. For any trajectory problem, the ultimate goal is an analytical solution (or at least an analytical approximation); however, there has yet to be any significant progress in generating a closed form solution for transfers to and from the vicinity of the libration points. The introduction of DST as a means of dynamical analysis and design in the three-body problem is motivated in part by the absence of analytical tools for transfer trajectories. Prior to using this approach, a trial and error numerical search method was most frequently used to design transfer trajectories. While this method has clearly been successful for various missions, a more elegant and efficient procedure is desirable. Application of DST in the

circular restricted three-body problem yields a relatively fast method of generating a number of different types of trajectories to and from halo orbits, e.g., transfers between Earth and halo orbits, and transfers between halo orbits in the vicinity of different libration points[5,8-12]. This success has led to the development of a utility based on DST to produce the much needed first guess that initiates the design process for transfer trajectories in more complicated models. An additional benefit of DST is a better understanding of the geometry of the phase space which then allows the mission designer to obtain valuable insight into the behavior of solutions in this particular region of space.

Investigations utilizing DST usually begin with special solutions. These might include equilibrium points, periodic orbits, quasi-periodic motions, and homoclinic as well as heteroclinic motions. Each of these solutions is an example of one of the fundamental models for the phase space, i.e., invariant manifolds. An $m-$dimensional manifold is analogous to a two-dimensional surface in $\mathbf{R}^n$. The concept of an invariant manifold can be simply described as follows: a collection of orbits that start on a surface and stay on that surface for the duration of their dynamical evolution. This basic definition can be used to characterize a variety of behaviors. In addition to the examples already mentioned, there exist invariant manifolds that asymptotically approach or depart other invariant manifolds. These are called stable and unstable manifolds, respectively.

In the circular three-body problem, the stable and unstable manifolds associated with periodic halo orbits have been the key to progress in the transfer problem (and the results can later be successfully extended to a more complex dynamic model). Note that an asymptotic approach to the target halo orbit renders a transfer to the halo orbit with no required insertion maneuver. While the task of developing expressions for these nonlinear surfaces is formidable, it is also unnecessary. The computation of the stable and unstable manifolds associated with a particular halo orbit can actually be accomplished numerically in a straightforward manner. The procedure used here is based on the monodromy matrix (the variational or state transition matrix after one period of the motion) associated with the halo orbit. This matrix essentially serves to define a discrete linear map of a fixed point in some arbitrary Poincaré section. As with any discrete mapping of a fixed point, the characteristics of the local geometry of the phase space can be determined from the eigenvalues and eigenvectors of the monodromy matrix. These are characteristic not only of the fixed point, but of the halo orbit itself.

The local approximation of the stable (unstable) manifold involves calculating the eigenvector of the monodromy matrix that is associated with the stable (unstable) eigenvalue, and then using the state transition matrix to propagate the approximation to any point along the orbit. The eigenvalues are known to be of the following form[4,5,8-12]:

$$\lambda_1 > 1 \ , \quad \lambda_2 = (1/\lambda_1) < 1 \ , \quad \lambda_3 = \lambda_4 = 1 \ ,$$
$$\lambda_5 = \lambda_6^* \ , \quad \text{and } |\lambda_5| = |\lambda_6| = 1 \ ,$$

where λ_5 and λ_6 are complex conjugates. Stable (and unstable) eigenspaces, E^s (E") are spanned by the eigenvectors whose eigenvalues have modulus less than one (modulus greater than one). There exist local stable and unstable manifolds, W^s_{loc} and W^u_{loc}, tangent to the eigenspaces at the fixed point, and of the same dimension[13,14]. Thus, for a fixed point $\bar{X}^H$ defined along the halo orbit, the one-dirneusional stable (unstable) manifold is approximated by the eigenvector associated with the eigenvalue λ_2 (A_i). First, consider the stable manifold. Let $\bar{Y}^{W^s}$ denote a six-dimensional vector that is coincident with the stable eigenvector and is scaled such that the elements corresponding to position in the phase space have been normalized. This vector serves as the local approximation to the stable manifold (W^s). Remove the fixed point $\bar{X}^H$ from the stable manifold to form two half-manifolds, W^{s^+} and IV'·Each half-manifold is itself a manifold consisting of a single trajectory. Now, consider some point $\bar{X}_o$ on W^{s^+}. Integrating both forward and backward in time from $\bar{X}_o$ produces W^{s^+} Thus, conceptually, calculating a half-manifold can be broken down into two steps: locating or approximating a point on W^{s^+}, and numerically integrating from this point.

To generate the stable manifold, an algorithm has been employed that was developed to find both the stable and unstable manifolds of a second order system[15]. The algorithm, however, does not possess any inherent limit to the order of the system, and has been used successfully here. Near the fixed point $\bar{X}^H$, W^{s^+} is determined, to first order, by the stable eigenvector $\bar{Y}^{W^s}$. The next step is then to globalize the stable manifold. This can be accomplished by numerically integrating backwards in time. It also requires an initial state that is on W^{s^+} but, not on the halo orbit. To determine such an initial state, the position of the spacecraft is displaced from the halo in the direction of $\bar{Y}^{W^s}$ by some distance d_s such that the new initial state, denoted as $\bar{X}_o^{W^s}$, is calculated as

$$\bar{X}_o^{W^s} = \bar{X}^H + d_s\, \bar{Y}^{W^s}. \tag{1}$$

Higher order expressions for $\bar{X}_o^{W^s}$ are available. but not necessary. The magnitude of the scalar d_s should be small enough to avoid violating the linear estimate, yet not so small that the time of flight becomes too large due to the asymptotic nature of the stable manifold. This investigation is conducted with a nominal value of 200 km for d_s. Note that a similar procedure can be used to approximate and generate the unstable manifold.

Application to Mission Design

Many stable and unstable manifolds for various halo orbits have been numerically generated in the circular problem to further understanding of the phase space. As an initial step in the design process, various types of these solution arcs are put together to construct a trajectory. Such an analysis produced the fundamental trajectory concept for GENESIS[12]. Two issues emerge that impact how the construction process proceeds. First, the initial approximation is ultimately used to generate a result in the "real" solar system; the methodology must accommodate this transition. Second, the design constraints may significantly influence the general size, shape, and overall characteristics of the trajectory. These constraints are loosely considered for the initial guess; they are tightly enforced in a later step.

Assumption *of Periodicity.* One of the fundamental characteristics that is exploited in applying DST to halo orbits in the circular problem is periodicity. The periodicity, however, is destroyed when movingto a dynamic model that includes ephemerides and other perturbations. Nevertheless, DST can still be very useful in the more complex models. The shift to a more complex model is facilitated by the selection of a quasi-periodic solution as the baseline orbit (even in the circular restricted problem) rather than an orbit that is precisely periodic. With the loss of periodicity, however, , two options are available for computations: 1) Compute stable and unstable manifolds for the tori on which the quasi-periodic trajectories are confined; 2) Assume that a Lissajous trajectory is sufficiently close to periodic that the algorithm discussed previously still provides an adequate approximation of the stable and unstable manifolds. Because the approximation from the previous section is only first order, and because the primary purpose in using the manifolds is to supply a first guess for some other numerical procedure, the second opt ion will suffice, i.e., assume a monodromy matrix exists and perform the calculations accordingly.

The next step requires definition of a period of motion for approximation of the monodromy matrix. For the simply periodic halo orbit, the period is (obviously) one revolution. In the case of a Lissajous trajectory, the motion more closely repeats after two revolutions. Because the motion is not precisely periodic, it is necessary to define the "beginning" and the "end" of one period. In this study, the '(beginning" of the period is defined at some specified xz-plane crossing, in the rotating coordinates, that is above the ecliptic plane (i.e., positive 2 direction). The "end" of the period is then defined at the xz-plane crossing two revolutions later. As an example, consider two revolutions of the Lissajous trajectory in Figure 1. Choose a period that originates at the Julian date 2452123.23 (near an xz-plane crossing). The duration of the period is 355.63 days which corresponds to two revolutions of the motion in the yz projection (see Figure 2). Consistent with the procedure

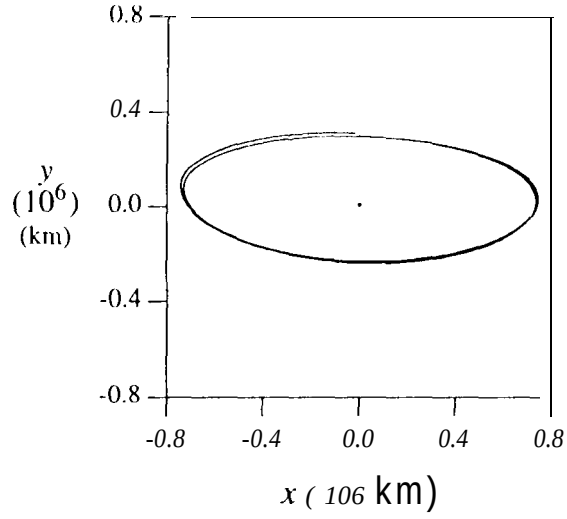

Figure 2 Assumed Period of the Motion for Generation of Stable Manifold

discussed previously, initial states $\bar{X}_o^{W^s}$ to generate the stable manifolds are computed along the corresponding two revolutions of the Lissajous.

Constraints. After generating the stable manifolds associated with various regions along the trajectory within the defined '(period", one particular region along the two revolution Lissajous can be identified that is associated with the stable manifolds that pass close to the Earth. Such a region along the Lissajous is visually indistinguishable from a similar region along a halo orbit[12]. In this region, there exists a stable manifold associated with a point very near the '(beginning" of the Lissajous trajectory; it passes the Earth at an altitude of 1112.1 km and an inclination of 15.3 degrees with respect to the equator. The date of the closest approach to the Earth is January 16, 2001 (within the desired time frame for the GENESIS launch). This serves as the initial guess for the transfer from Earth to the Lissajous trajectory.

The return portion of the trajectory, i.e., the transfer from the L_1 Lissajous trajectory to Earth return, can be considered in much the same way. Recall that, since a day-side reentry is required, a direct return from L_1 is not feasible. The spacecraft must approach reentry from the side of the Earth opposite the Sun. Therefore, an *unstable* manifold must be generated that approaches the L_2 region before returning to Earth. It must also depart the vicinity of L_1 only after sufficient time to perform the science investigations has elapsed. Thus, further downstream along the same quasi-periodic Lissajous orbit, two revolutions are defined to represent the new "period" for computation of an appropriate unstable manifold. In this case, the period originates on Julian date 2452300.34, again near an xz-crossing. The resulting two revolution interval is 356.03 days in duration. Investigation of the unstable manifolds along different regions of the appropriate revolutions reveals a region where the corresponding unstable manifolds have the characteristics necessary for the return. Specifically, an unstable manifold is required that reaches L_2 (comparable to a heteroclinic type motion); the trajectory then must pass close to the Earth. One such path returns to the Earth at an altitude of 197.4 km with an inclination of .52.1 degrees and a declination of 35.8 degrees on August 21, 2003. Combining the stable manifold as the launch segment, the Lissajous trajectory, and the unstable manifold as the return segment provides the first guess for an end-to-end solution in the real system (that is, the model using ephemerides) for the GENESIS mission. Note that the full model may also include additional perturbations, such as solar radiation pressure. Each of the three trajectory arcs are plotted in Figure 3 with an "o" marking the locations w'here the arcs are patched together.

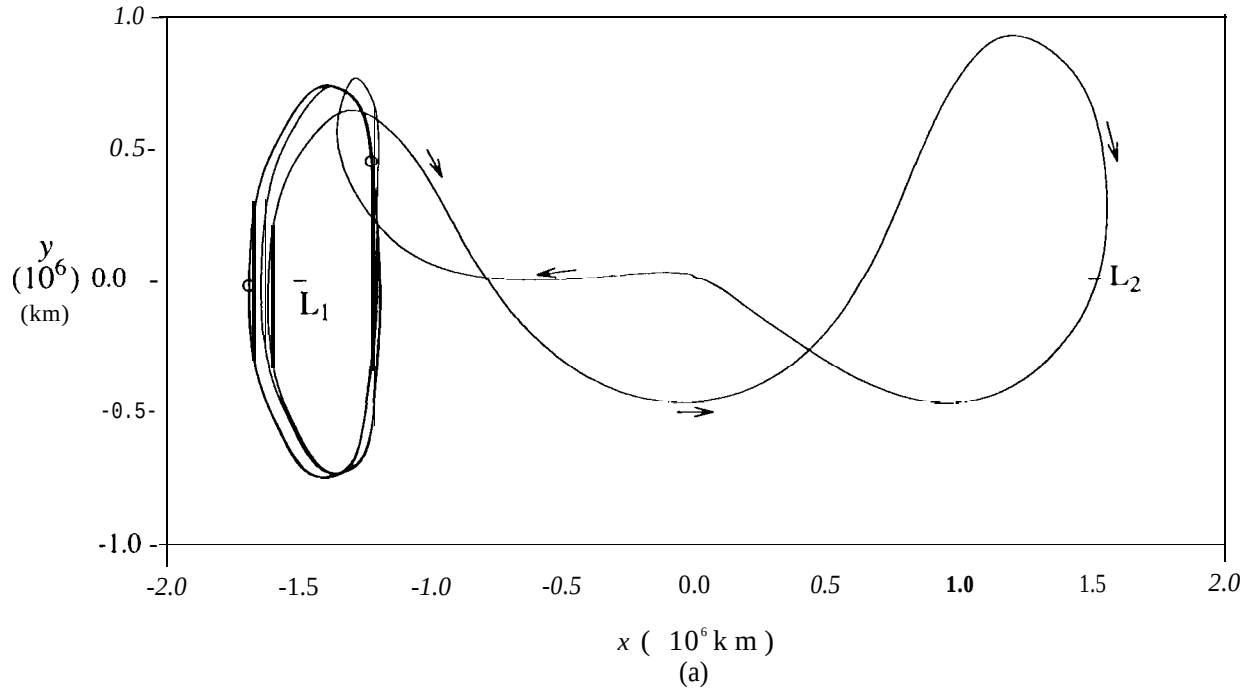

(a)

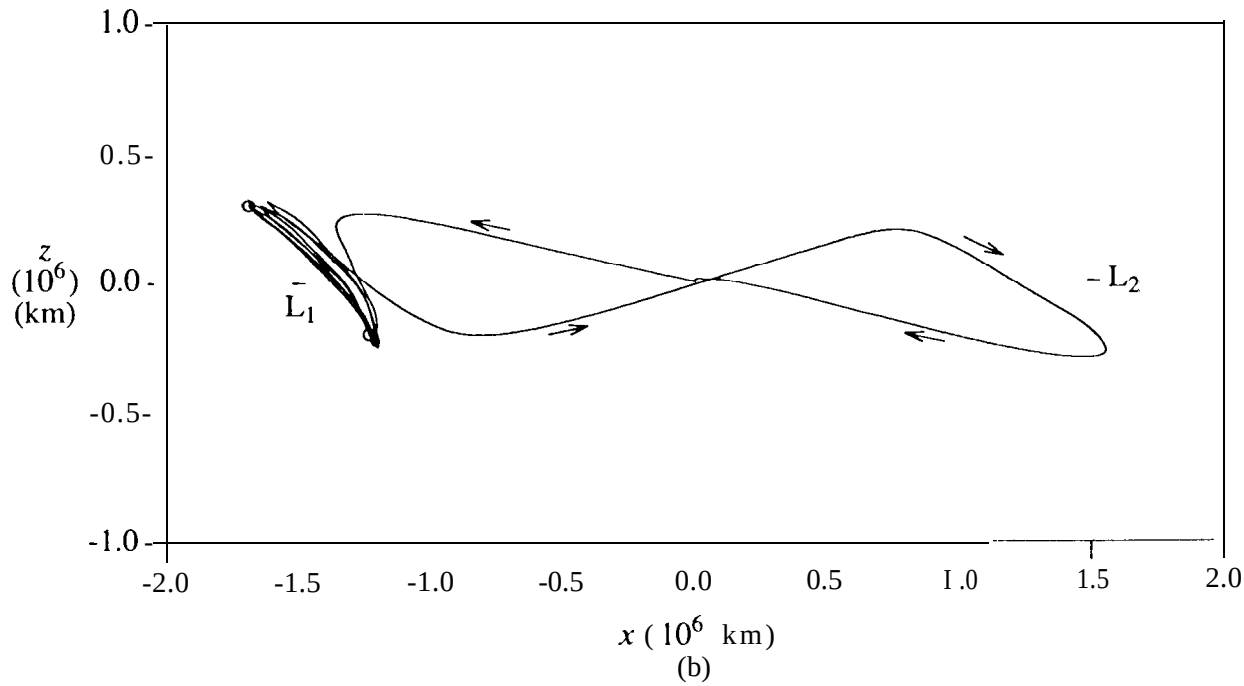

(b)

Figure 3 **Initial Guess Generated Using Dynamical Systems** Theory

MEETING LAUNCH/RETURN CONSTRAINTS

The next step is to use the initial guess obtained previously to begin the search for a viable solution that rigorously meets the various constraints placed on the trajectory. To accomplish this task, the trajectory is decomposed into multiple segments. Each segment will be considered separately, but will be analyzed similarly. Thus, the solution process for each segment is generalized. In particular, both the launch and the return segments have specified constraints that must be met near the Earth, and both segments have one end state! away from the Earth that is fixed in position and time. So, the problem on each segment is formulated in terms of a fixed position and time as one end state and some set of launch or return conditions near the Earth as the other end state. While the launch and return constraints are specified in terms of different variables, the basic methodology presented here works equally well for both cases.

Methodology

The methodology for enforcing the constraints (denoted generally as the scalar quantities α_k) and ensuring a viable solution is identical to that described in Wilson and Howell[16], and Howell and Wilson[17]. The solution is discretized into a series of patch points with states defined along the trajectory. To generate a reference, the patch point positions and times are temporarily frozen. Between each pair of patch points, an arc is determined, essentially the solution to an n-body Lambert problem between consecutive patch points. At this stage, the trajectory has position and time continuity; however, effective velocity discontinuities may now exist at each patch point (excluding the initial and final states). The current estimate of the outgoing velocity state ($\bar{V}_n^+$) at any patch point n is compared with the incoming velocity state ($\bar{V}_n^-$) to compute the patch point velocity discontinuities, that is, $\Delta\bar{V}_n = \bar{V}_n^+ - \bar{V}_n^-$. (Note that these patch point $\Delta\bar{V}$'s are represented in terms of inertial coordinates.) The subscript n denotes the patch point number ordered sequentially along the trajectory beginning with the initial state. The patch point states themselves are also expressed using the n-subscript convention. By varying the patch point state positions and times in a specified manner, the resulting AV'S can be eliminated or significantly reduced, and the constraints α_k can be satisfied, while the desired characteristics of the solution are retained. It is significant that this is a two stage procedure: position continuity, then simultaneous reduction of any effective velocity discontinuities. (See the methodology in Howell and Pernicka[7].)

To employ a differential corrections process to reduce the total cost, it is necessary to derive the relationships between any $\Delta\bar{V}_n$ or constraint α_k, and the independent variables in the problem. Since the trajectory is described in terms of discrete patch point positions and times, it is convenient to select these quantities as the independent parameters. Therefore, it is necessary to determine the variation of each $\Delta\bar{V}_n$ and constraint α_k due to variations in the patch point positions and times, which have thus far been fixed at values determined during the initial approximation. A linear relationship between these states can be represented in matrix form as

$$\begin{Bmatrix} \delta\Delta\bar{V}_n \\ \delta\alpha_k \end{Bmatrix} = [M] \begin{Bmatrix} \delta\bar{R}_j \\ \delta t_j \end{Bmatrix} \quad , \tag{2}$$

where

$$[M] = \begin{bmatrix} \frac{\partial\Delta\bar{V}_n}{\partial\bar{R}_j} & \frac{\partial\Delta\bar{V}_n}{\partial t_j} \\ \frac{\partial\alpha_k}{\partial\bar{R}_j} & \frac{\partial\alpha_k}{\partial t_j} \end{bmatrix} \quad , \tag{3}$$

and $\bar{R}_j$ and t_j denote the position and time corresponding to the j^{th} patch point,. Notice that the matrix $[M]$ (called the State Relationship Matrix or SRM) is not square, that is, there are more independent variables ($\bar{R}_j$ and t_j) than there are dependent variables ($\Delta\bar{V}_n$ and α_k). Since this system is underdetermined, there are infinitely many solutions, and it is therefore possible to estimate the changes in the values of the independent variables that are necessary to reduce $\Delta\bar{V}_n$ and

α_k, and thus, the total cost. Note that if, through the addition of constraints, the system becomes overdetermined, it is still possible to add flexibility and maintain the underdetermined nature by including additional patch points in the analysis. The number of patch points and their placement is currently a function of experience and numerical experimentation. Although the size of the SRM can be large, this disadvantage is offset by the fact that state transition matrices (STMs), generated in conjunction with the various trajectory segments, are available and can be used to produce expressions for each partial in the matrix[16,18].

From Wilson and Howell[16], the non-zero variations of $\Delta\bar{V}_n$ with respect to the positions $\bar{R}_j$ are expressed

$$\frac{\partial \Delta \bar{V}_n}{\partial \bar{R}_{n-1}} = -B_{n-1,\,n}^{-1}\,, \tag{4}$$

$$\frac{\partial \Delta \bar{V}_n}{\partial \bar{R}_n} = -B_{n+1,n}^{-1} A_{n+1,n} + B_{n-1,n}^{-1} A_{n-1,\,n}\,, \tag{5}$$

$$\frac{\partial \Delta \bar{V}_n}{\partial \bar{R}_{n+1}} = B_{n+1,n}^{-1}\,. \tag{6}$$

where the STMS ($[\Phi_{n,n-1}]$ and $[\Phi_{n+1,n}]$) surrounding the patch point n are written in terms of four 3 x 3 submatrices; for example,

$$[\Phi_{n,n-1}] = \begin{bmatrix} \frac{\partial \bar{R}_n}{\partial \bar{R}_{n-1}} & \frac{\partial \bar{R}_n}{\partial \bar{V}_{n-1}^{+}} \\ \frac{\partial \bar{V}_n^{-}}{\partial \bar{R}_{n-1}} & \frac{\partial \bar{V}_n^{-}}{\partial \bar{V}_{n-1}^{+}} \end{bmatrix} = \begin{bmatrix} A_{n,n-1} & B_{n,n-1} \\ C_{n,n-1} & D_{n,n-1} \end{bmatrix}. \tag{7}$$

The partials of $\Delta\bar{V}_n$ with respect to all other patch point positions can be shown to be zero, since the velocities at any given patch point are related only to the trajectory segments surrounding it. Similarly, the non-zero variations of $\Delta\bar{V}_n$ with respect to the times t_j are evaluated as follows[16]

$$\frac{\partial \Delta \bar{V}_n}{\partial t_{n-1}} = B_{n-1\,n}^{-1}\,\bar{V}_{n-1}^{+}\,, \tag{8}$$

$$\frac{\partial \Delta \bar{V}_n}{\partial \bar{R}_n} = B_{n+1,n}^{-1} A_{n+1,n}\,\bar{V}_n^{+} - B_{n-1,n}^{-1} A_{n-1,n} \bar{V}_n^{-}\,, \tag{9}$$

$$\frac{\partial \Delta \bar{V}_n}{\partial t_{n+1}} = -B_{n+1,n}^{-1} \bar{V}_{n+1}^{-}\,. \tag{10}$$

Again, the partials of $\Delta\bar{V}_n$ with respect to the other patch point times are zero.

In order to incorporate constraints into the solution process, it is necessary to determine the variations of α_k with respect to variations in the independent parameters. The launch constraints for GENESIS include a departure from a circular parking orbit with an altitude of 200 krn and an inclination of 28.5 degrees. The appropriate partials and the targeting process are described in detail in Howell and Wilson[17]. The return conditions are slightly more complex. The planned retrieval of the spacecraft is to occur at the Utah Test ancl Training Range (UTTR). So, the spacecraft targets specific coordinates on a rotating Earth, i.e., a declination of 40.6 degrees and a right ascension of -114.0 degrees, corresponding to UTTR. The atmospheric part of the reentry trajectory will not be considered in this analysis. Instead, an altitude of 125 km and a flight path angle of -7.9 degrees is targeted. However, in this study, the flight path angle constraint is transformed into a constraint on true anomaly (where a value of 344.5 degrees results in a flight path angle approximately equal to the -7.9 degrees that is required to reenter). The partial derivatives for each of these constraints

can be derived as follows, beginning with altitude.

Since altitude is related to the independent parameters through the magnitude of the position vector R, the scalar constraint can be writ ten as

$$\alpha_1 = |\bar{R}| - R_{des} \quad , \tag{11}$$

where R_{des} is the desired altitude. Thus, the variation is expressed in the form

$$\frac{\partial \alpha_1}{\partial \bar{R}} = \frac{\bar{R}^T}{|\bar{R}|} \quad . \tag{12}$$

Note that the partial with respect to time is zero

For declination and right ascension, it is desired to target a specific location on the rotating (non-inertial) Earth. Define then a set of cartesian coordinates fixed in the Earth, such that $\hat{z}_{bf}$ is coincident at all times with the axis of rotation of the Earth and assumed constant. The $\hat{x}_{bf}$ unit vector is defined along the Greenwich meridian and $\hat{y}_{bf}$ completes the orthonormal triad. The declination can thus be evaluated as

$$\sin \quad (decl) \frac{\mathbf{R} \cdot \hat{z}_{bf}}{|\bar{R}|} \quad , \tag{13}$$

where the symbol "·" represents the inner product. The right ascension is computed as

$$rt.asc = \arctan\left(\frac{\bar{R} \cdot \hat{y}_{bf}}{\bar{R} \cdot \hat{x}_{bf}}\right) \tag{14}$$

As an approximation, we, the rotation rate of the Earth about $\hat{z}_{bf}$ is assumed constant. Therefore, the expression for declination is only a function of the position vector R, and the only non-zero partial in the SRM is

$$\frac{\partial \sin\ (decl)}{\partial \bar{R}} = \frac{1}{|\bar{R}|} \left[\hat{z}_{bf}^T \right] \quad (decl) \quad \frac{\bar{R}^T}{|\bar{R}|} \tag{15}$$

Although $\hat{z}_{bf}$ is assumed constant, the directions of $\hat{x}_{bf}$ and $\hat{y}_{bf}$ change with respect to the inertial frame as the Earth rotates, so right ascension is a function of position R as well as time t. The partial derivative of right ascension with respect to R produces

$$\frac{\partial rt.asc}{\partial \bar{R}} = \frac{1}{\left[1 + \frac{\bar{R} \cdot \hat{y}_{bf}}{\bar{R} \cdot \hat{x}_{bf}}\right]^2} \frac{\partial}{\partial \bar{R}} \left(\frac{\bar{R} \cdot \hat{y}_{bf}}{\bar{R} \cdot \hat{x}_{bf}}\right) \tag{16}$$

$$= \frac{\left(\bar{R} \cdot \hat{x}_{bf}\right) \hat{y}_{bf}^T - \left(\bar{R} \cdot \hat{y}_{bf}\right) \hat{x}_{bf}^T}{\left(\bar{R} \cdot \hat{x}_{bf}\right)^2 + \left(\bar{R} \cdot \hat{y}_{bf}\right)^2} \quad . \tag{17}$$

Similarly, the partial with respect to time is expressed

$$\frac{\partial rt.asc}{\partial t} = \frac{1}{\left[1 + \frac{\bar{R} \cdot \hat{y}_{bf}}{\bar{R} \cdot \hat{x}_{bf}}\right]^2} \frac{\partial}{\partial t} \left(\frac{\bar{R} \cdot \hat{y}_{bf}}{\bar{R} \cdot \hat{x}_{bf}}\right) \quad . \tag{18}$$

From the previous assumption that ω_e is constant, the time derivatives can be written in the forms

$$\frac{\partial \hat{x}_{bf}}{\partial t} = -\omega_e \hat{y}_{bf} \quad \text{and} \quad \frac{\partial \hat{y}_{bf}}{\partial t} = \omega_e \hat{x}_{bf} \quad , \tag{19}$$

so that, ultimately, the partial of right ascension with respect to time reduces to

$$\frac{\partial rt.asc}{\partial t} = \omega_e \quad . \tag{20}$$

All tile necessary partials in matrix [M] are, thus, available.

As noted, the system is underdetermined, and the SRM in Equation (2) is not invertible. Out of all possible changes in positions and times, choose the set with the smallest Euclidean norm, that is,

$$\left\{ \begin{array}{c} \delta \bar{R}_j \\ \delta t_j \end{array} \right\} = [M]^T \left([M][M]^T \right)^{-1} \left\{ \begin{array}{c} \delta \Delta \bar{V}_n \\ \delta \alpha_k \end{array} \right\} , \tag{21}$$

where the differential changes in $\Delta \bar{V}_n$ and α_k are selected to reduce the total cost. This process is iterative and continues until the cost is minimized to within some specifier tolerance.

Nominal Solution for January

The actual design can now proceed. As previously mentioned, the algorithm is currently formulated to manage one end state that is free (perhaps near the Earth) and one end state that is fixed in position and time, so it is necessary to consider the GENESIS trajectory in multiple segments. The break points between segments depend on the various possible constraints for the mission. A natural place to break the trajectory is at the set of maneuver points, i.e., AV'S. For this particular mission, there is a requirement that there be a minimum time interval of 23 months without a significant maneuver (due to potential contamination of the science experiments by the thrusters). Because of this constraint, it is desirable that the Lissajous orbit insertion (LOI) maneuver occur as soon as possible. To accommodate this requirement, the location for LOI is selected, somewhat arbitrarily, to be at the first xz-plane crossing (below the ecliptic). This location also serves as a natural choice to break the trajectory.

The first guess for the launch segment (the segment from the Earth to LOI) is taken directly from the first part of the stable manifold that was generated previously. Of course, the complete stable manifold extends beyond the specified LOI location by approximately one-half revolution. The differential corrections process then yields a solution that is continuous in position and velocity and departs an Earth parking orbit (with the specified conditions) on January 15, 2001.

The next segment of the trajectory is the intermediate leg that includes the portion of the stable manifold beyond LOI and the Lissajous trajectory. The position and time at LOI is held fixed for the intermediate leg. The corrections algorithm then quickly generates a smooth (in position and velocity) trajectory segment from the LOI point to the beginning of the unstable manifold that was previously generated. At this point, there are velocity discontiuuities at both ends of this intermediate section. However, without having met the return constraints, the specific magnitudes are meaningless.

The final step in the process is blending the intermediate leg and the unstable manifold together as the second segment of the trajectory. Recalling that a minimum of 23 months after LOI is required before another maneuver, the next significant AV is placed at the xz-plane crossing after the spacecraft leaves the vicinity of L_1 along the unstable manifold (nearly mid-way between the Earth and L_1). In addition, another maneuver is allowed to occur near the L_2 point. This provides some flexibility before the final approach toward Earth, and it adds additional control over the trajectory. To accommodate these maneuvers, deterministic AV'S must be possible at *any* patch point. In Equation (21), rather than the usual procedure to eliminate all AI "s, the velocity discontinuity at

any patch point can be driven to a specified magnitude, and the corresponding differential change is

$$\delta\Delta\bar{V}_n = \frac{\|\Delta V_{des}\| - \|\Delta\bar{V}_n\|}{\|\Delta\bar{V}_n\|} \cdot \Delta\bar{V}_n \quad , \tag{22}$$

where ΔV_{des} is the desired deterministic maneuver.

With this modification, the second segment of the trajectory is computed using the arcs discussed earlier as an initial guess and allowing maneuvers at the specified locations. The final result of this process is an end-to-end trajectory with three maneuvers (the 1.01 maneuver and the two AV'S in the return segment) that meets all of the specified constraints on launch and return. The end-to-end trajectory is plotted in Figure 4 and is summarized in Table 1. It is important to note that this solution is not necessarily optimal. In the current formulation, the location and time of the LOI point are essentially additional constraints on the solution introduced by the design process.

Table 1
GENESIS Trajectory Summary for Nominal January Launch

Event	Date (m/d/y)	Altitude (km)	ΔV (m/s)
Earth Launch	01/15/01	200	3193.82
LOI	05/03/01		5.20
Maneuver	03/30/03		20.00
Maneuver	06/11/03		20.00
Reentry	08/21/03	125	

Multiple Reentry Opportunities

As mentioned previously, the nominal strategy is to target a specified reentry state. However, a decision can be made one day prior to the nominal reentry to abort. In this case, a maneuver must be executed to raise perigee sufficiently to avoid reentering the atmosphere (a flyover perigee specified to be approximately 200 km altitude). Once this is completed and the spacecraft reaches perigee, another maneuver must be implemented for capture into a 16 day Earth-centered orbit. When the spacecraft reaches the apogee of this orbit, another maneuver retargets the spacecraft for a second reentry opportunity at the same coordinates (onthe rotating Earth). The reentry can again be aborted one day prior to the second reentry pass. Thcstrategy for a third and final reentry opportunity is the same (witbout the need for a maneuver at perigee to capture). A close up of the three reentry opportunities appears in Figure 5, with the symbol "o" indicating the maneuver locations. The costs for both scenarios are summarized in Table 2.

Table 2
GENESIS Trajectory Summary for Additional Reentry Opportunities

	Second Reentry			Third Reentry		
Event	Date (m/d/y)	Altitude	ΔV (111/s)	Date (111/d/y)	Altitude (km)	ΔV (m/s)
Deflection	08/20/03		7.59	09/06/03		4.87
Perigee	08/21/03		38.50	09/07/03		*0.00*
Apogee	08/30/03		28.32	09/15/03		11.50
Reentry	09/07/03	125		09/23/03	125	

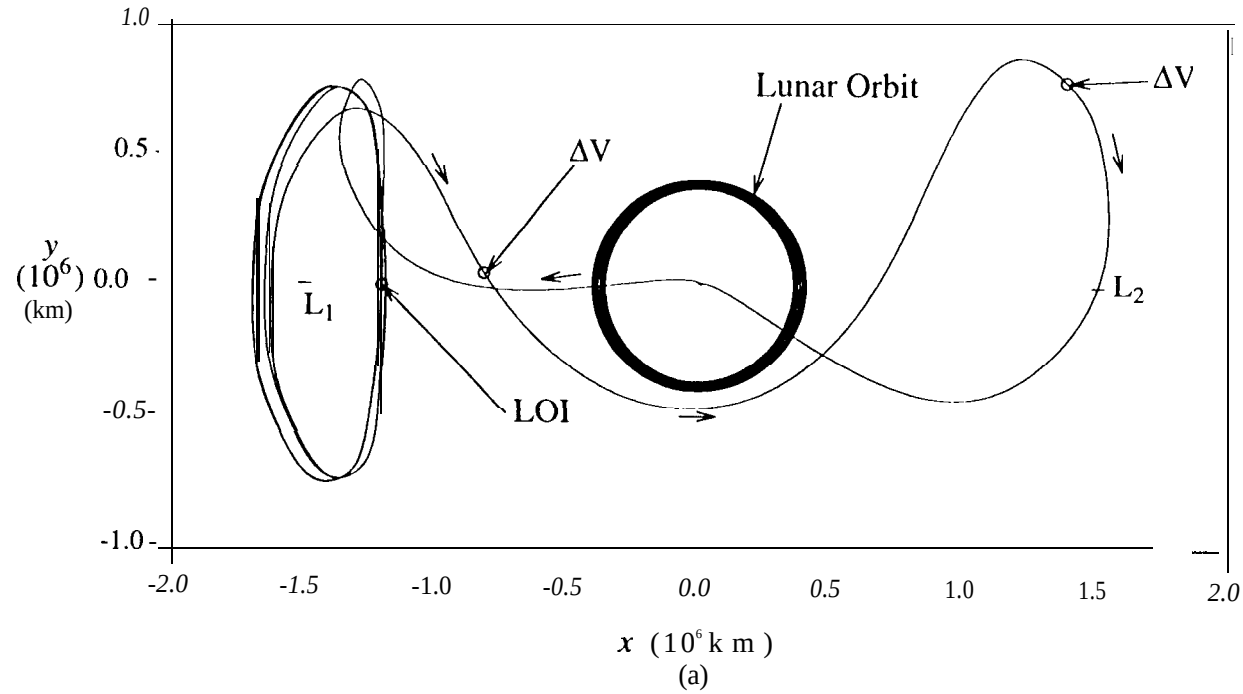

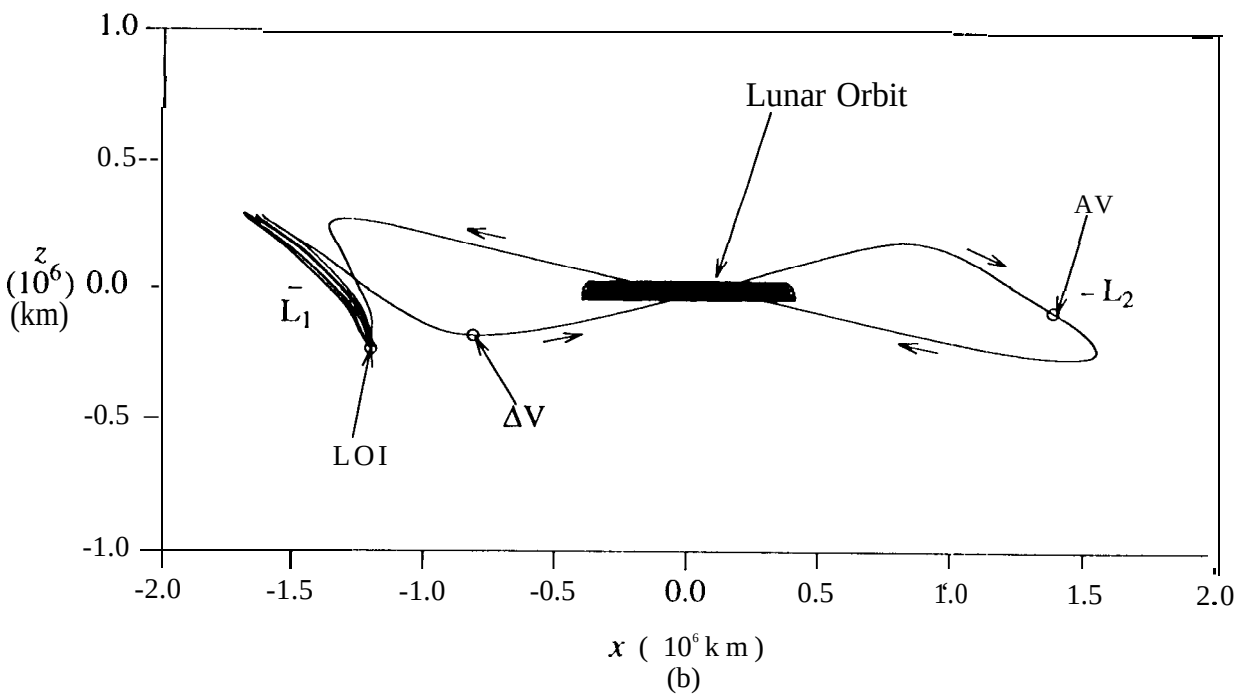

Figure 4 Nominal GENESIS Solution with January 15, 2001 Launch

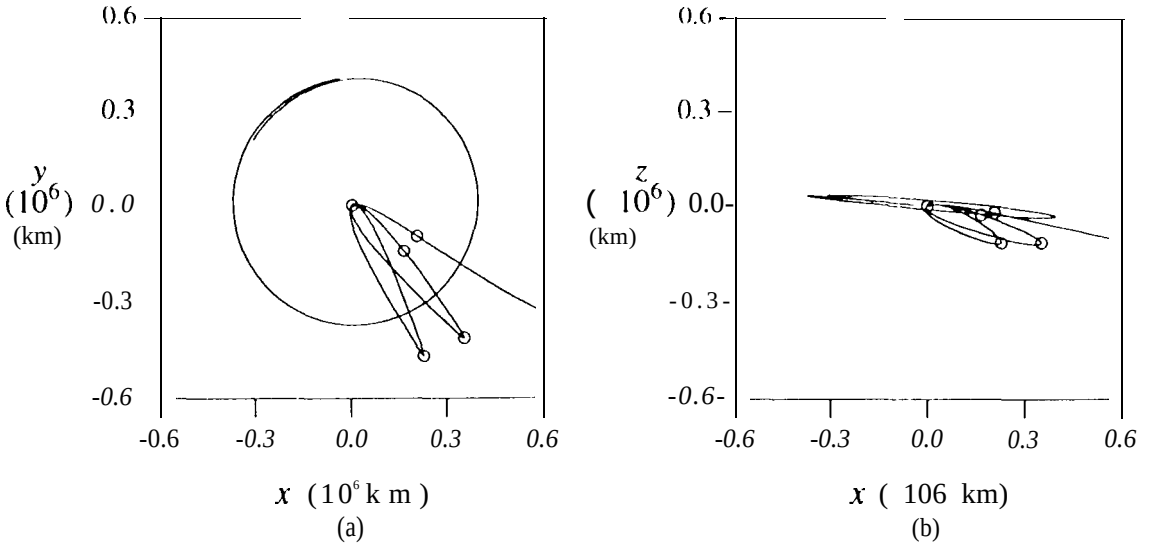

Figure 5 Three Reentry Opportunities

EXPLORING OTHER LAUNCH OPPORTUNITIES

There are essentially two aspects involved in exploring the possibility of multiple launch opportunities. The first is the standard launch period analysis, where solutions are sought over a number of clays surrounding the nominal launch. In addition, launch opportunities are also sought in other months as well. Specifically, additional solutions are required with launches in the months of December 2000 and February 2001. The previous process can be repeated; it is straightforward and individual steps are automated. However, another simpler approach can be used for this part of the analysis.

Launch Opportunities in Other Months

often in the three-body problem, the key to successfully understanding a problem is to view the shape of the solution in rotating coordinates. The significance of halo orbits, for example, is apparent only in the rotating frame. In the case of GENESIS, preserving the shape of the solution in the rotating frame is critical. To accomplish this, patch points along the nominal solution are first transformed from the inertial frame to an appropriate rotating frame. The rotating frame of choice is dependent on the location of the patch point. Specifically, patch points that are near L_1 are transformed to rotating libration point coordinates relative to L_1, those near L_2 are transformed to rotating Ii brat ion point coordinates relative to L_2, and those near the Earth are transformed in to Sun- Earth rotating coordinates relative to the Earth. Next, the date associated with the patch point state is advanced 28 days for February or slipped 28 days for December (based on the approximate period of the Moon in the respective rotating frame). The states are then t ransformed back into inertial coordinates using the adjusted times. These inertial states then serve as the initial estimate for the patch point states in the new months. This provides a sufficient first guess that quickly leads to solutions in both months. Both solutions are summarized in Table 3.

Launch Period Analysis for Each Case

The strategy for the launch period analysis comes in part from the intuition gained in investigat- iug the unstable manifolds, and also from experience. The primary issue that drives the methodology

Table 3
GENESIS Trajectory Summary for December and February Launches

	December			February		
Event	Date (m/d/y)	Altitude (km)	ΔV (m/s)	Date (m/d/y)	Altitude (km)	ΔV (m/s)
Earth Launch	12/18/00	200	-3194.56	02/12/01	200	3193.22
LOI	04/05/01		42.69	05/31/01		10.08
Maneuver	03/02/03		17.57	04/27/03		*20.00*
Maneuver	05/04/03		19.99	07/08/03		*19.41*
Reentry	07/24/03	125	_	09/18/03	125	

is the sensitivity of the return portion of the trajectory. A very slight change in the state near L_1 can result in escape from the vicinity of the Earth, or perhaps a return to Earth thousands of kilometers off target. In addition, the position of the *Moon* as the spacecraft passes from L_1 toward L_2 can have a significant impact. Therefore, the strategy for the launch period analysis begins by freezing the return segment of the trajectory. More specifically, only the initial launch segment need be analyzed. So, in addition to the usual launch constraints, an additional time constraint in the form of a specified Julian date is placed on the launch state. 'I'he AV budget for the trajectory from launch to the first reentry (excluding trajectory correction maneuvers) is assumed to be 90 m/s. The duration of the launch period is then determined by computing solutions with varying launch dates until the required AV at the LOI point, plus the other deterministic AV's in the various nominal solutions, surpasses the 90 m/s total. The results of this analysis are presented in Figure 6 where the nominal solutions for each month (computed in the previous section) are marked with the symbol "o". The data for the curves iuthis figure are computedb yadjusting the launch dates at oneday increments. However, there are no constraints that would prohibit continual launch opportunities from the specified parking orbit throughout the launch periods in each of the three months.

Of additional interest here is the observation that two local minimums appear during each month. In each case, the minimum with the larger magnitude corresponds to the dynamical situation where the spacecraft passe closer -to the Moon than in any other solution option during that samemonth. For most of the cases in all three months, the closest lunar encounter during the launch segment ranges from a spacecraft-lunar distance of 300,000 km to 400,000 km. In the region of the higher local minimum, the spacecraft passes much closer to the Moon; within 83,000 km for December, 106,000 km for January, and 124,000 km for February. For various reasons, it is specified that a lunar encounter is to be avoided for GENESIS. Nonetheless, the Moon's impact is clear, and it could potentially be useful if a lunar encounter were incorporated into the launch strategy.

CONCLUSIONS

The goal of this study (aside from the actual mission design) isdernonstration of the advantages to be gained by using dynamical systems theory in the design process. In particular, DST can be directly applied to the more complex dynamical models in spite of the loss of periodicity of the orbit relative to the libration point. In addition to the first guess utility, a great deal of insight can be gained that is valuable throughout the design process. This is demonstrated in the formulation of the launch period analysis. Also apparent is a certain degree of symmetry in the procedure to satisfy launch and return constraints. In each of the cases investigated, the successor the design, both in meeting the mission constraints and in efficiency of the design process, is based on an improved theoretical understanding of the three body problem.

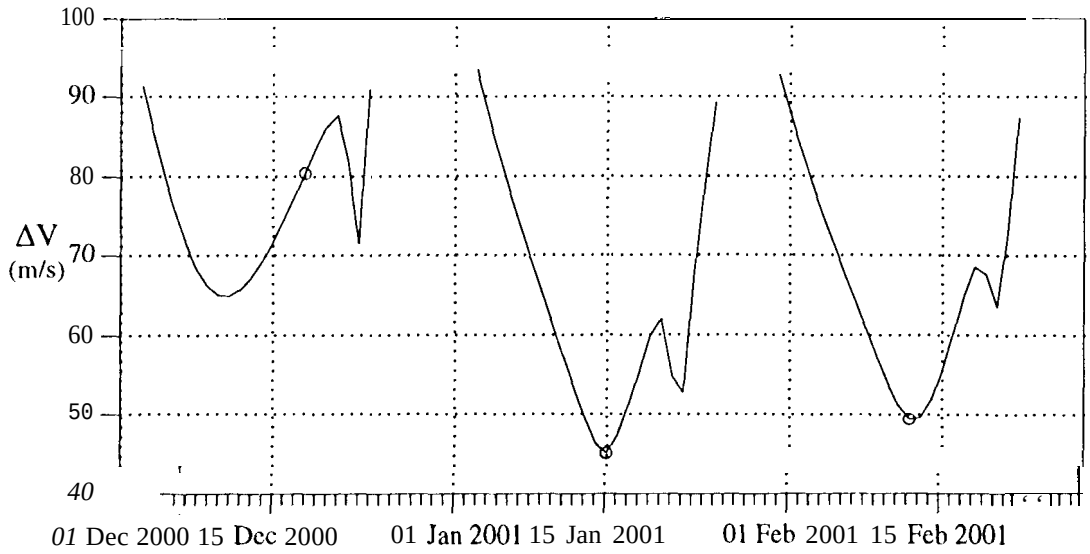

Figure 6 Launch Period Analysis

ACKNOWLEDGMENTS

Portions of this work were carried out at the Jet Propulsion Laboratory, California Institute of Technology, and at Purdue University, under a contract with the National Aeronautics and Space Administration. This effort has also been supported by NASA under Award Number NCC7-5.

References

[1] D. L. Richardson, "Analytic Construction of Periodic Orbits About the Collinear Points," *Celestial Mechanics,* Vol. 22, 1980, pp. 241-253.

[2] D. L. Richardson and N. D. Cary, "A Uniformly Valid Solution for Motion About the Interior Libration Point of the Perturbed Elliptic-Restricted Problem," AAS Paper 75-021, *AIAA/AAS Astrodynamics Specialists Conference,* Nassau, Bahamas, July 1975.

[3] R. W. Farquhar, "The Control and Use of Libration-Point Satellites," Goddard Space Flight Center, Technical Report, September 1970.

[4] K. C. Howell, "Three-Dinlensional, Periodic, 'Halo' Orbits," *Celestial Mechanics,* Vol. 32, 1984, pp. 53--71.

[5] K. C. Howell, D. L. Mains, and B. T. Barden, "Transfer Trajectories From Earth Parking Orbits to Sun-Earth Halo Orbits," AAS Paper 94-160, *AIAA/AAS Spaceflight Mechanics Meeting,* Cocoa Beach, Florida, February 1994.

[6] P. Sharer, H. Franz, and D. Folta, "Wind Trajectory Design and Control," *CNES International symposium on Space Dynamics,* Toulouse, France, June 1995.

[7] K. C. Howell and H. J. Pernicka, "Numerical Determination of Lissajous Trajectories in the Restricted Three-Body Problem, " *Celestial Mechanics, Vol.* 41, 1988, pp. 107-124.

[8] G. Gómez, A. Jorba, J. Masdemont, and C. Simó, "Final Report: Study Refinement of Semi-Analytical Halo Orbit Theory," ESOC Contract Report, Technical Report, April 1991

[9] G. Gómez, A. Jorba, J. Masdemont, and C. Simó, "Study of the Transfer from the Earth to a Halo Orbit Around the Equilibrium Point L_1," Technical Report, December 1991.

[10] G. Gómez, A. Jorba, J. Masdemont, and C. Simó, "Moon's Influence on the Transfer from the Earth to a Halo Orbit Around L_1," Technical Report.

[11] B. 1. Barden, "Using Stable Manifolds to Generate 'Transfers in the Circular Restricted Problem of Three Bodies," M.S. Thesis, School of Aeronautics and Astronautics, Purdue University, West Lafayette, Indiana, December 1994.

[12] B. T. Barden, K. C. Howell, and M. W. Lo, "Application of Dynamical Systems Theory to Trajectory Design for a Libration Point Mission," *Journal of the Astronautical Sciences,* Vol. 45, No. 2, 1997 (to appear).

[13] J. Guckenheimer and P. Holmes, *Nonlinear oscillations, Dynamical Systems, and* Bifurcations *of Vector Fields. New* York: Springer-Verlag, 1983.

[14] S. Wiggins, *Introduction to Applied Nonlinear Dynamical Systems and Chaos.* New York: Springer-Verlag, 1990.

[15] T. S. Parker and L. 0. Chua, *Practical Numerical Algorithms for Chaotic Systems. New* York: Springer-Verlag, 1989.

[16] R. S. Wilson and K. C. Howell, "A Design Concept for Multiple Lunar Swingby Trajectories," AIAA Paper 94-3718, *AIAA/AAS Astrodynamics Conference,* Scottsdale, Arizona, August 1994.

[17] K. C. Howell and R. S. Wilson, "'Trajectory Design in the Sun-Earth-Moon System Using Multiple Lunar Gravity Assists," AIAA Paper 96-3642, *AIAA/AAS Astrodynamics Conference,* San Diego, California, August 1996.

[18] R. S. Wilson, "A Design Tool for Constructing Multiple Lunar Swingby Trajectories," M.S. Thesis, Purdue University, December 1993.

APPENDIX: A SECOND EXAMPLE

It is notable in this problem that the solution space is complex and not yet fully explored. A second example demonstrates a lower-cost alternative; perhaps more importantly, however, it suggests some structure underlying a potential family of solutions. This second result is obtained using the initial guess that was previously generated using DST. However, the reduction algorithm to meet the launch/return constraints is implemented with a slight variation. The LOI point is shifted further back, i.e., closer to the launch by 9.5 days. With exactly the same launch and return constraints, the solution converges to the trajectory in Figure A.1 and Tables A.1 and A.2. The solution appears very similar to the result in the previous example (Figure 4). However, the *only* significant AV is the LOI maneuver. In the current formulation, the location and time of the LOI point is effectively a constraint. By shifting the point along the manifold, the algorithm converged to a solution with a somewhat higher LOI AV but a zero-cost return segment.

It is also observed that the algorithm has adjusted the Lissajous to be slightly larger (notably in the A_y direction). As seen in Table A.2, the cost for additional reentry opportunities is approximately the same. This second baseline solution for January can now be relatively easily extended to the other months. The new launch period analysis appears in Figure A.2, and is compared with that

from the previous example. Assuming that the larger Lissajous trajectory is acceptable, the figure illustrates continuous launch opportunities over the three months at a lower total cost. More in-depth analysis is ongoing.

Table A.1
Trajectory Summary for Lower-Cost January Launch

Event	Date (m/d/y)	Altitude (km)	ΔV (m/s)
Earth Launch	01/15/01	200	3193.76
LOI	04/23/01		8.47
Reentry	08/19/03	125	

Table A.2
Trajectory Summary for Additional Reentry Opportunities

	Second Reentry			Third Reentry		
Event	Date (m/d/y)	Altitude (km)		Date (m/d/y)	Altitude (km)	ΔV (m/s)
Deflection	08/18/03			09/06/03		7.09
Perigee	08/19/03			09/07/03		0.00
Apogee	08/29/03			09/16/03		15.18
Reentry	09/07/03	125		09/25/03	125	

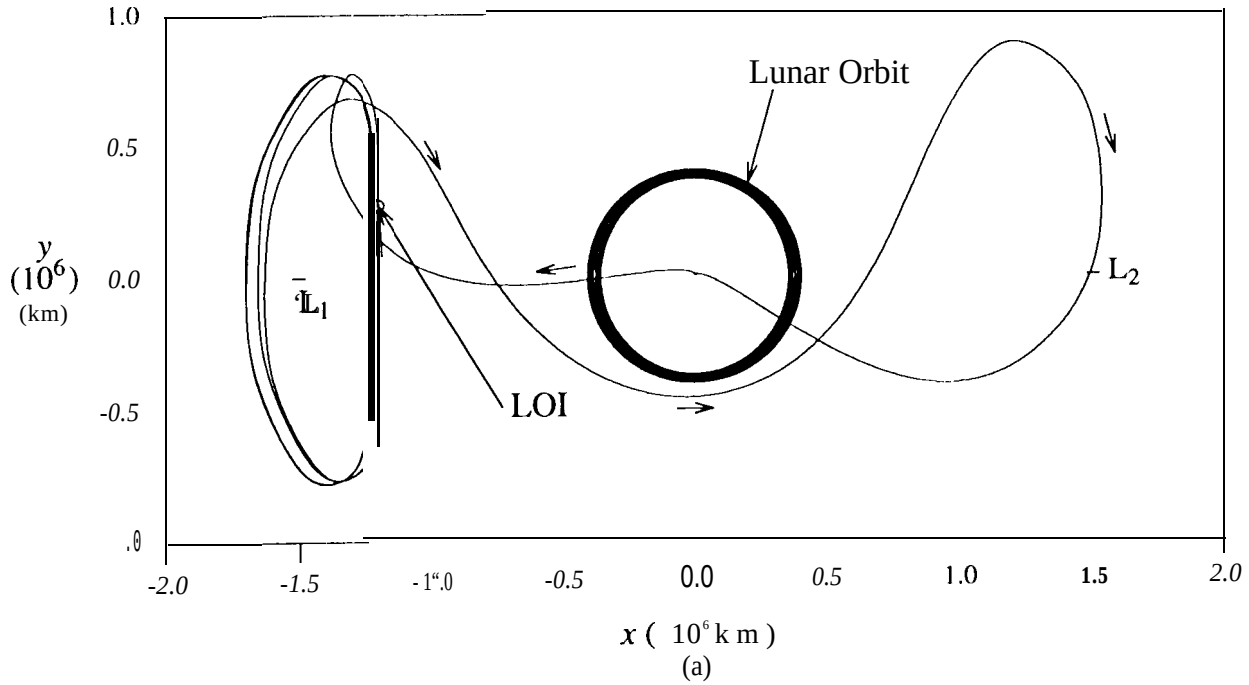

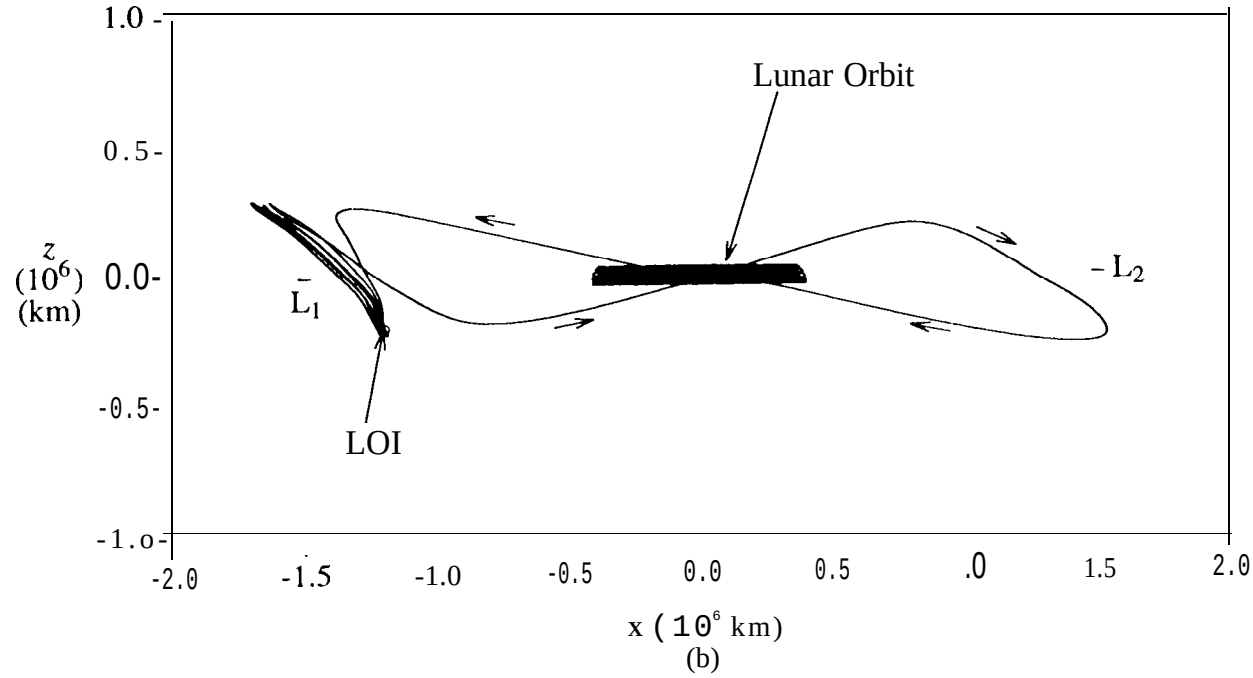

Figure A.1 Lower-Cost Solution with January 15, 2001 Launch